Near-infrared nano-spectroscopy and emission energy control of semiconductor quantum dots using a phase-change material

Nobuhiro Tsumori, [1] Motoki Takahashi, [1] Nurrul Syafawati Humam, [1] Phillipe Regreny, [2] Michel Gendry[2] and Toshiharu Saiki [1]

[1] Graduate School of Science and Technology, Keio University, 3-14-1 Hiyoshi, Kohoku-ku, Yokohama-shi, Kanagawa 223-8522, Japan
[2] Université de Lyon, Institut des Nanotechnologies de Lyon, UMR-CNRS 5270, Ecole Centrale de Lyon, 69134 Ecully, France

Email: saiki@elec.keio.ac.jp

Abstract. We have proposed a method to achieve near-field imaging spectroscopy of single semiconductor quantum dots with high sensitivity by using an optical mask layer of a phase-change material. Sequential formation and elimination of an amorphous aperture allows imaging spectroscopy with high spatial resolution and high collection efficiency. We present numerical simulation and experimental result that show the effectiveness of this technique. Inspired by this optical mask effect, a new approach which can precisely control the emission energy of semiconductor quantum dots has been proposed. This method uses the volume expansion of a phase change material upon amorphization, which allows reversible emission energy tuning of quantum dots. A photoluminescence spectroscopy of single quantum dots and simulation were conducted to demonstrate and further explore the feasibility of this method.

1. Introduction

Semiconductor quantum dots (QDs) have shown great promise as efficient single photon emitters and entangled photon sources, making them attractive for quantum communication and quantum information processing applications. Self-assembled InAs QDs on InP substrates are promising as near-infrared (NIR) single photon and entangled photon emitters [1-3]. In order to clarify and control the optical properties of QDs for telecommunication devices, photoluminescence (PL) spectroscopy studies of single QDs with high spatial resolution at NIR wavelength is necessary. The most useful technique to attain this is by using near-field scanning optical miscroscopy (NSOM) [4-6]. The advantage of NSOM is its ability to perform imaging spectroscopy of single QDs with a spatial resolution determined by the aperture size without the need to process the sample. On the other hand, NSOM has a lower PL collection efficiency at NIR wavelength than at visible wavelength. The transmission efficiency of NIR radiation through the aperture decreases inversely with about the sixth power of the wavelength [7]. This problem inhibits NIR-PL spectroscopy based on NSOM to be practically realized. Therefore, we proposed a method to overcome the low NIR-PL spectroscopy by using a nanoaperture on an optical mask layer of phase-change material (PCM).

PCM mask effect has also the potential to be applied in emission energy control of QDs. One of the main problems for realization of quantum communication applications is the precise control of the emission energy of QDs. The three main existing approaches to tune emission energy include

externally applied magnetic field [8], electric field [9] and mechanical strain [10, 11]. The magnetic field method is believed to be the most promising approach in tuning energy over a wide range; however, large equipment is required. Electric field method allows one to tune emission energy over a large range, however, significant decrease in excitonic emission intensity was observed with a high electric field. Mechanical stress method can in principle be used to tune energy; however, the energy tuning range is still limited. In addition, another drawback of the current techniques is they have not shown precise energy control of individual QDs. Scanning probe miscroscopy (SPM) allows a spatially local perturbation with nanoscale resolution [11-13]; however, this technique requires a feedback control mechanism, making it mechanically unstable and impractical. As a modified method of nanoindentation with a probe tip, we proposed a new approach to precisely control the emission energy of QDs by applying local strain using volume expansion of phase-change material. In this study, we experimentally demonstrate and further explore the feasibility of our proposed method.

This paper is organized as follows. Section 2 presents the principles, mainly focusing on the properties of phase-change material. Section 3 shows the sample and measurement setup used in experimental studies. Section 4 demonstrates the numerical simulation and experimental results for near-infrared nano-spectroscopy of QDs using a phase-change mask layer. We show that an amorphous nanoaperture allows imaging spectroscopy with high spatial resolution and high collection efficiency. Section 5 focuses on the experimental and simulation results of emission energy control of QDs using volume expansion of a phase-change material. We show that this approach can serve as a method which allows reversible energy tuning of individual QDs.

2. Principles

A phase-change material (PCM) is a substance that is widely used for rewritable data storage applications. A PCM can be transformed from crystalline phase to amorphous phase, and vice versa, by laser pulse irradiation. When a short pulse of a high intensity laser beam heats the crystalline region above the melting point, it is melted and rapidly quenched into the amorphous phase. Longer and weaker pulse heating to a temperature above the glass transition temperature leads to the transition of amorphous phase to crystalline state. The large optical contrast between amorphous state and crystalline state is advantageous for recording media applications. One of the most prominent examples of a PCM is GeSbTe (GST).

The idea of PCM mask layer has been implemented by Tominaga *et al.* in super-resolution near field structure disk for high-density optical data storage [14]. According to reference [15], $Ge_2Sb_2Te_5$ has high optical contrast at excitation wavelengths of 600nm-900nm which allows aperture-size dependent resolution, and also has low extinction coefficient at telecommunication wavelength of 1550nm which results in high collection efficiency. These features are essential in measuring photoluminescence of quantum dots. Figure 1 illustrates the schematic diagram of nanospectroscopy using a PCM mask.

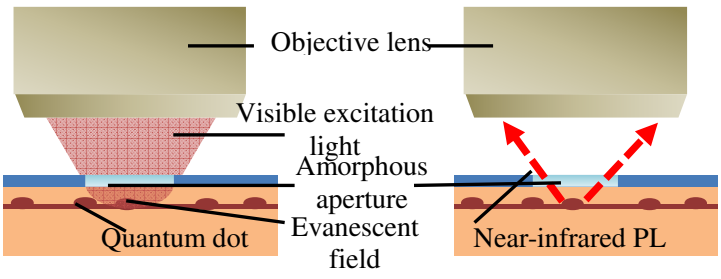

Figure 1. Schematic diagram of a phase-change mask layer above QDs.

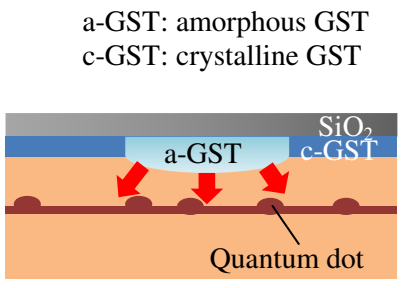

Figure 2. Schematic illustration of strain induced QDs using volume expansion of a GST layer.

A focused laser beam forms a local amorphous region in the crystalline GST film. Approximately 10% volume expansion accompanies the transformation from crystalline phase to amorphous phase. Following the theoretical prediction that volume of PCM should increase upon amorphization, stress can be induced on QDs and cause energy shift. This stress is released when amorphous phase is transformed into crystalline phase using laser annealing. The magnitude of energy shift can be controlled because the amorphized volume is proportional to the number of laser pulses during irradiation. Figure 2 shows the schematic diagram of compressive strain to individual QDs by local amorphization of a GST layer.

3. Experimental details

3.1 Sample growth

Low density self-assembled double-capped InAs/InP QDs grown by solid-source molecular beam epitaxy (SSMBE) were used as sample for our experimental studies. 250nm thick InP buffer layer was deposited on semi-insulating InP(001) substrate at 600^{o}C. The temperature was then reduced to 500^{o}C. Self-assembled InAs QDs were formed on InP surface by using double capping method. 1.4ML of InAs was deposited on InP surface. Then, a thin InP layer (2nm), also known as first cap layer, was grown on the QDs. After that, 120s growth interruption occurred under P_2 flow, where As/P exchange occurred. Temperature was increased to 600^{o}C and the structure was then capped with another InP layer (100nm), also known as InP second cap. Finally, a $Ge_2Sb_2Te_5$ (GST) film layer, was deposited directly on the whole structure to a thickness of 40nm, followed by a 50nm thick SiO_2 layer by sputtering. The SiO_2 layer acts as a protective layer.

3.2 Micro-photoluminescence measurement setup

We used micro-photoluminescence (μPL) measurement to investigate the emission properties of QDs in the experiments. All measurements were conducted at low temperature. The sample was first placed on the cold finger of a helium flow cryostat, ensuring temperature below 10K. During the PL measurement, QDs were excited using a He-Ne laser (λ=632.8nm) or a CW laser (λ=662nm) through a spot, and PL signal was detected by a spectrometer and a liquid-nitrogen cooled InGaAs diode array.

4. Near-infrared nano-spectroscopy of QDs using a phase-change mask layer

4.1 Numerical simulation

The performance of the PCM mask method was evaluated by conducting simulation focusing on the spatial resolution aspect. We calculated three-dimensional electromagnetic field distributions in the vicinity of the amorphous aperture by employing finite-difference time-domain (FDTD) method. We simulated the illumination profile obtained using a focused visible light beam (λ=633 nm). Figure 3(a) presents a schematic diagram of the model. In this model, a crystalline $Ge_{10}Sb_2Te_{13}$ film (c-GST) with 50nm thickness was coated as a mask layer on a bulk InP substrate (refractive index n=3.2). $Ge_{10}Sb_2Te_{13}$ has a refractive index of n=3.16 + 4.24i at wavelength, λ=633 nm. At the centre of the mask layer, an amorphous aperture (a-GST) with a diameter of 300 nm was formed and the aperture was illuminated using x-polarized focused light. The simulation volume was 4×4×4 μm^3.

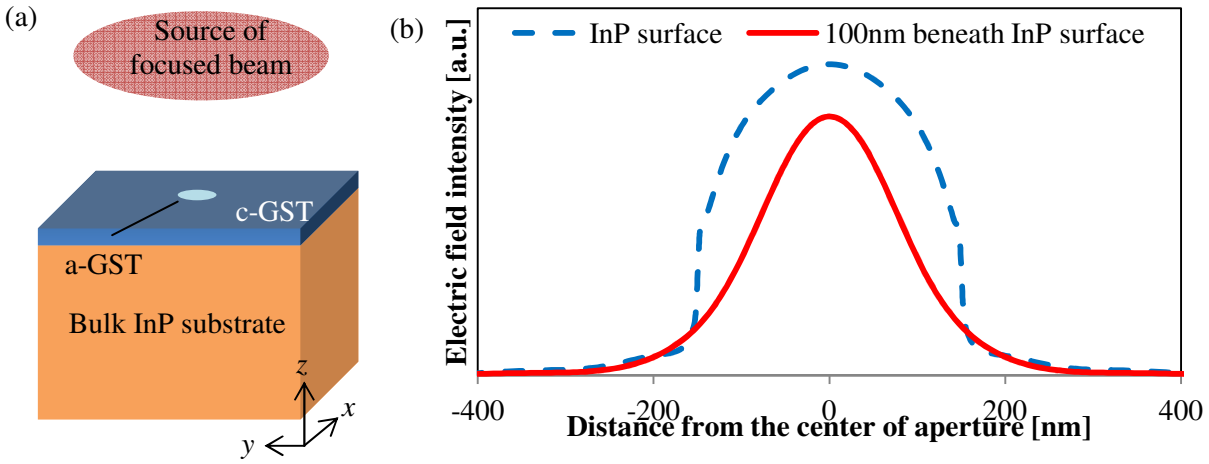

Figure 3.(a) Schematic of calculation model for illumination using a focused beam,(b) Cross-sectional profiles of electric field intensity (*xy* -plane) at the InP surface and at 100nm beneath InP surface

Figure 3(b) shows the cross-sectional profiles of electric field intensity in the *xy*-plane calculated at two points; at InP surface and at depth of 100nm beneath the InP surface. By calculating the full widths at half maximum (FWHM) of each profile, the illumination area at a depth of 100nm below surface (FWHM=190nm) is significantly smaller than the illumination area just below the aperture (FWHM=280nm). This is attributed to the large refractive index of InP which provides a higher spatial resolution than the diameter of aperture.

4.2 Experiment

An amorphous aperture was formed by irradiating the GeSbTe mask with 10 femtosecond laser pulses (λ=800 nm) at a fluence of 27 mJ/cm^2 through a microscope objective (NA=0.8). The diameter of the amorphous region was approximately 300 nm based on confocal laser scanning microscopy measurement. A laser diode (λ=662 nm) was used to recrystallize the amorphous aperture by thermal annealing. During PL measurement, a He–Ne laser was focused onto the amorphous aperture through a microscope objective (NA=0.65) at excitation wavelength 632.8nm. PL spectrum was measured using spectromenter and a liquid-nitrogen-cooled InGaAs photodiode array.

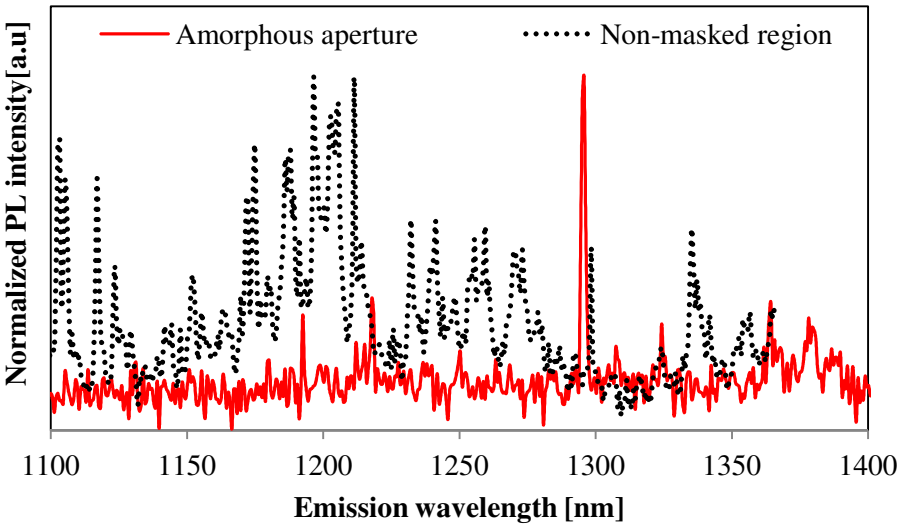

Figure 4. PL spectra of InAs QDs obtained through the amorphous aperture (solid line) and non-masked region (dotted line).

Figure 4 compares the PL spectra of InAs QDs through the amorphous aperture (solid line) and non-masked region (dotted line). In the region without mask layer, one can observe a spectrum with many peaks, which corresponds to an ensemble of QDs. Based on the spatial resolution of measurement and the number of peaks, the QD density of used sample was estimated to be $3.3\times 10^9/cm^2$. On the contrary, the spectrum obtained through the amorphous aperture shows only one peak as a result of large reduction in area of observation. The number of peaks obtained agrees well with the estimated QD density and the size of amorphous aperture. This result demonstrates that the amorphous mask can serve as an aperture which allows high spatial resolution without degrading the collection efficiency of PL signal.

4. Local control of emission energy of QDs using volume expansion of a phase-change material

4.1 Experiment

Nanoscale amorphization was performed by irradiation of a subnanosecond Q-switched solid state laser. Here, a nanosecond Q-switched laser was focused through a microscope objective lense (N.A=0.65) at excitation wavelength 532nm onto the sample surface. During the PL measurement, QDs were excited using a CW laser at excitation wavelength 662nm through the amorphous aperture, and PL signal was detected by a spectrometer and a liquid-nitrogen cooled InGaAs diode array. For local crystallization, a semiconductor nanosecond pulsed laser (λ=662 nm) was used. Crystallization and amorphization processes were repeated and changes in PL peak energy shift were observed. An amorphous region with a diameter of approximately 1 μm was formed under the conditions of the laser wavelength (532 nm) and microscope objective (NA=0.65).

Figure 5 shows the PL spectra of QDs obtained after crystallization and re-amorphization of GST film. The GST film is in the amorphous state at point A and point C, and crystalline state at point B. Redshift was observed after amorphization, and its recovery to its original position was observed after recrystallization. This indicates that this method allows reversible energy tuning of the emission from individual QDs. The maximum energy shift obtained during experiment was approximately 2.3meV. A wider energy shift range is expected by manipulating the thickness of GST film.

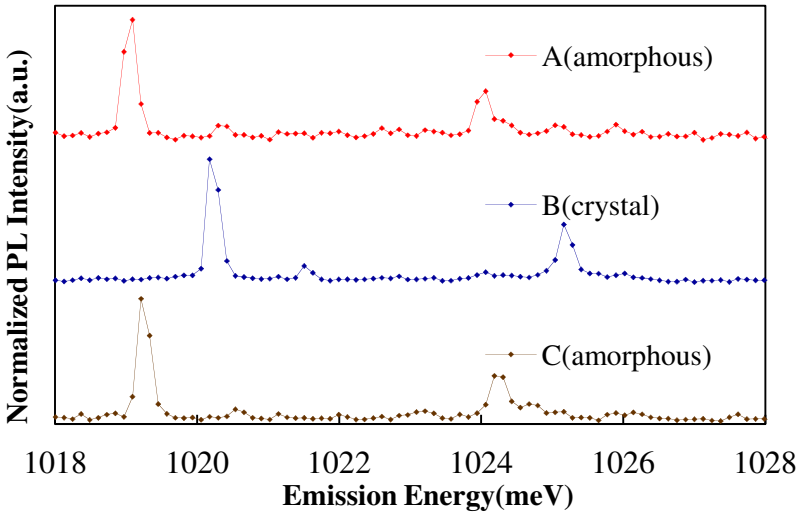

Figure 5. PL spectra of QDs obtained as a result of local amorphization and crystallization of GST film

4.2 Simulation

We developed a two-dimensional finite element (FE) model to investigate the stress distribution and energy shift distribution in the sample. Since the proposed method is considered as a modified approach to nanoindentation with a probe tip, we conducted an indentation test using ANSYS 14.0 simulation software. The geometry of the model is illustrated in Figure 6.

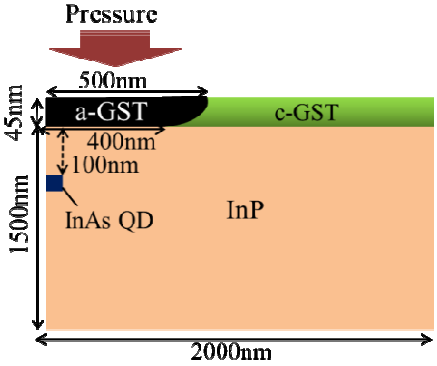

Figure 6. Geometry of model used in calculation

Indentation was simulated assuming the apex of the indenter applies compressive stress on the top of InP surface. The size of the indenter is selected based on the amorphous mark size obtained in experiment. A quantum dot (InAs QD) with width of 20nm and height of 1nm was placed 100nm below the surface of the sample along *y*-axis. These values are taken based on the microscopic observation of the QD sample used in experiment. Young's modulus and Poisson's ratio of InP, InAs and $Ge_{10}Sb_2Te_{13}$ are listed in Table 1. According to our previous experimental results, amorphization of phase change material caused approximately 2meV redshift of PL peak energy. The indentation force was chosen to generate a 2meV redshift at 100nm beneath the top of InP surface.

Table 1. List of material parameters used in calculation

material	InP	InAs	$Ge_{10}Sb_2Te_{13}$ (amorphous)	$Ge_{10}Sb_2Te_{13}$ (crystal)
Young's modulus (Pa)	6.10×10^{10}	5.14×10^{10}	2.02×10^{10}	3.00×10^{10}
Poisson's ratio	0.30	0.36	0.33	0.30

The energy shift was calculated by using the following equation [16], which provides the shift of QD emission energy induced by [001] compression.

$$\Delta E_{e-hh} = \frac{a}{Y}(1-2\nu)3\sigma^h + \frac{2b}{Y}(1+\nu)\frac{3}{2}\sigma^u_{zz} \quad (1)$$

where Y and ν are Young's modulus and Poisson's ratio respectively. $\sigma^h = \frac{1}{3}(\sigma_{xx}+\sigma_{yy}+\sigma_{zz})$ and $\sigma^u_{zz} = \sigma_{zz} - \sigma^h$ correspond to mean stress components and deviatoric stress components respectively. The value of a and b is obtained from Reference [17]. The first term in Equation (1) shows the energy shift due to hydrostatic stress, while the second term in Equation (1) corresponds to the energy shift due to uniaxial stress.

Figure 7 shows the stress distribution in the model obtained through finite element modelling (FEM) simulation. In this model, the indentation force is approximately 100MPa and the stress applied on the QD is at least 50MPa. The energy shift distribution in our model obtained through calculation is

illustrated in Figure 8. The energy shift is negative (redshift) at the shallow area beneath the flat part of indenter. On the contrary, the energy shift is positive (blueshift) beneath the edge region of indenter. In previous experiments, we obtained both redshift and blueshift after a local amorphization of GST film. The ratio of redshift and blueshift obtained was 11:2. This simulation result agrees well with our previous experimental results which show both redshift and blueshift as a result of compressive stress applied by volume expansion of phase change material.

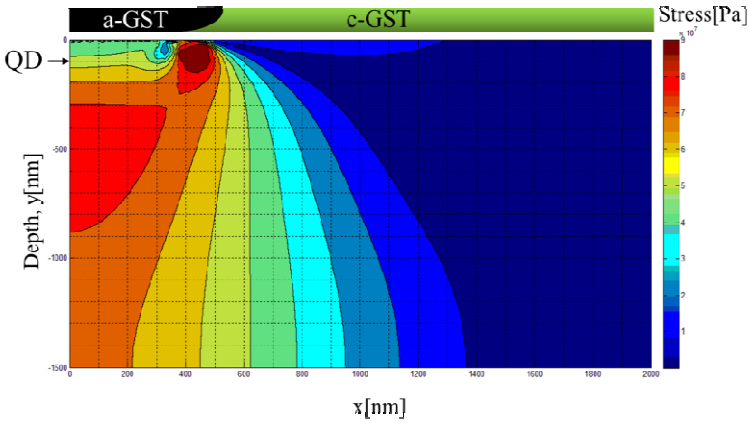

Figure 7. Stress distribution in model.

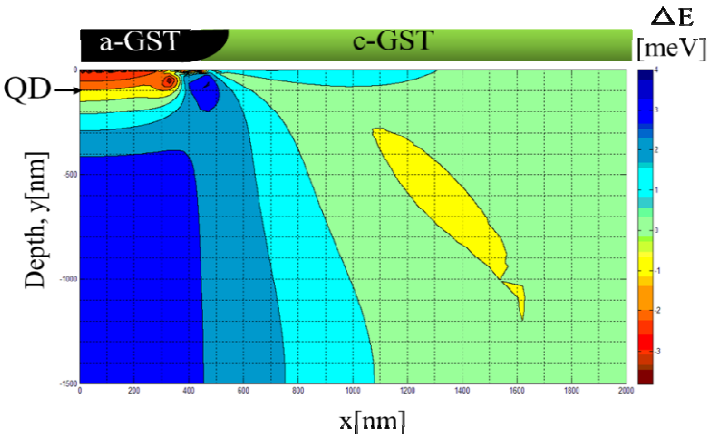

Figure 8. Energy shift distribution in model.

5. Conclusion

We have demonstrated the feasibility of near-field imaging spectroscopy with a phase-change mask layer by performing numerical simulation and PL measurements of QDs. We report that the amorphous mark can act as an aperture; reducing the observation area without degrading the collection efficiency of PL signal. We have also experimentally demonstrated the ability of our method to tune the energy of emission from QDs. Significant shifts in emission energy of QDs indicate that effective emission energy control can be realized through this method. We also showed that this technique allows reversible energy tuning. These results can be used for imaging spectroscopy and energy tuning purposes which is crucial for realizing quantum communication applications.

Acknowledgements

We acknowledge the Ministry of Education, Culture, Science and Technology Japan for financial support; Grant-in-Aid for Scientific Research(B). We would like to thank Keiichiro Yusu for depositing GeSbTe film on the QDs.

References

[1] Takemoto K, Nambu Y, Miyazawa T, Wakui K, Hirose S, Usuki T, Takatsu M, Yokoyama N, Yoshino K, Tomita A, Yorozu S, Sakuma Y and Arakawa Y 2010 *Appl. Phys. Express* **3** 092802
[2] Miyazawa T, Takemoto K, Sakuma Y, Hirose S, Usuki T, Yokoyama N, Takatsu M and Arakawa Y 2006 *Jpn. J. Appl. Phys.* **44** L620
[3] Bimberg D, Stock E, Lochmann A, Schliwa A, Tofflinger JA, Unrau W, Munnix M, Rodt S, Haisler VA, Toropov AI, Bakarov A and Kalagin AK 2009 *IEEE Photonics J.* **1** 58
[4] Saiki T, Nishi K and Ohtsu M 1998 *Jpn. J. Appl. Phys., Part 1* **37** 1638
[5] Matsuda K, Saiki T, Nomura S, Mihara M and Aoyagi Y 2002 *Appl. Phys. Lett.* **81** 2291
[6] Sugimoto Y, Tsumori N, Saiki T and Nomura S 2009 *Opt. Rev.* **16** 269
[7] Tsumori N, Takahashi M, Sakuma Y and Saiki T 2011 *Appl. Opt.* **50** 5710
[8] Stevenson RM, Young RJ, See P, Gevaux DG, Cooper K, Atkinson P, Farrer I, Ritchie DA and Shields AJ 2006 *Phys. Rev. B* **73** 033306
[9] Kowalik K, Krebs O, Lemaitre A, Laurent S, Senellart P and Voison P 2005 *Appl. Phys. Lett.* **86** 041907
[10] Seidl S, Kroner M, Hogele A, Karrai K, Warburton RJ, Badolato A and Petroff PM 2006 *Appl. Phys. Lett.* **88** 203113
[11] Robinson HD, Muller MG, Goldberg BB and Merz JL 1998 *Appl. Phys. Lett.* **72** 2081
[12] Bhallamudi VP, Berger AJ, Labanowski DE, Stroud D and Hammel PC 2012 *J. Appl. Phys.* **111** 013902
[13] Mei E and Higgins DA 1998 *J. Phys. Chem. A* **102** 7758-7563
[14] Tominaga J, Suji H, Sato A, Nakano T, Fukaya T and Atoda N 1998 *Jpn. J. Appl. Phys.* **37** L1323-L1325
[15] Strand D, Tsu DV, Miller R, Hennessey M and Jablonski D 2006, contributed paper presented at European Phase Change and Ovonics
[16] Mintairov AM, Sun K, Merz JL, Li C, Vlasov AS, Vinokurov DA, Kovalenkov OV, Tokranov V and Oktyabrsky S 2004 *Phys. Rev B* **69** 155306
[17] Priester C, Allan G and Lannoo M 1988 *Phys. Rev. B* **37** 8519